

# Express delivery of fossil meteorites from the inner asteroid belt to Sweden

David Nesvorný <sup>a,\*</sup>, David Vokrouhlický <sup>a</sup>, William F. Bottke <sup>a</sup>, Brett Gladman <sup>b</sup>,  
Therese Häggström <sup>c</sup>

<sup>a</sup> Department of Space Studies, Southwest Research Institute, 1050 Walnut St., Suite 400, Boulder, CO 80302, USA

<sup>b</sup> Department of Physics and Astronomy, University of British Columbia, 6224 Agricultural Road, Vancouver, BC, V6T 1Z1, Canada

<sup>c</sup> Department of Earth Sciences, Marine Geology, Göteborg University, P.O. Box 460, SE-405 30 Göteborg, Sweden

Received 26 August 2006; revised 23 October 2006

Available online 10 January 2007

## Abstract

Our understanding of planet formation depends in fundamental ways on what we learn by analyzing the composition, mineralogy, and petrology of meteorites. Yet, it is difficult to deduce the compositional and thermal gradients that existed in the solar nebula from the meteoritic record because, in most cases, we do not know where meteorites with different chemical and isotopic signatures originated. Here we developed a model that tracks the orbits of meteoroid-sized objects as they evolve from the  $\nu_6$  secular resonance to Earth-crossing orbits. We apply this model to determining the number of meteorites accreted on the Earth immediately after a collisional disruption of a  $D \sim 200$ -km-diameter inner-main-belt asteroid in the Flora family region. We show that this event could produce fossil chondrite meteorites found in an  $\approx 470$  Myr old marine limestone quarry in southern Sweden, the L-chondrite meteorites with shock ages  $\approx 470$  Myr falling on the Earth today, as well as asteroid-sized fragments in the Flora family. To explain the measured short cosmic-ray exposure ages of fossil meteorites our model requires that the meteoroid-sized fragments were launched at speeds  $> 500 \text{ m s}^{-1}$  and/or the collisional lifetimes of these objects were much shorter immediately after the breakup event than they are today.

© 2007 Elsevier Inc. All rights reserved.

**Keywords:** Meteorites; Asteroids; Asteroids, dynamics

## 1. Introduction

Meteorites are hand-samples of their parent bodies (mostly asteroids) that have survived passage through our atmosphere to reach the Earth's surface. The oldest meteorite specimens are remnants of the first geologic processes to occur in our Solar System 4.6 byr ago. Properly analyzed, the composition, mineralogy, and petrology of meteorites can be used to constrain planet formation processes as well as the evolution of the solar nebula. One fundamental difficulty with interpreting the meteorite record, however, is that we do not know (with a few exceptions) the location of their parent planetary bodies (or their immediate precursors). Determining the linkages between meteorites and their parent bodies is therefore a critical goal of asteroid and meteoritic studies.

Studies show that meteoroids, the meter-sized precursors of the meteorites, are delivered to Earth via a three-step process: (1) Main-belt asteroids collide with one another at high speeds and undergo fragmentation (Bottke et al., 2005a, 2005b). (2) Fragments undergo dynamical evolution via the Yarkovsky effect (Vokrouhlický and Farinella, 2000), a thermal radiation force that causes objects to undergo semimajor axis drift, and reach locations of powerful resonances produced by the gravitational perturbations with the planets (e.g., the 3:1 and  $\nu_6$  resonances). (3) Meteoroids placed in such resonances have their eccentricities pumped up (e.g., Wetherill and Williams, 1979; Wisdom, 1982, 1985) to the point that objects become planet-crossing. A small fraction of these bodies go on to strike Earth (Gladman et al., 1997), though most impact the Sun or are ejected from the inner Solar System by Jupiter (Farinella et al., 1994).

An important clue to determine the immediate source region of meteoroids is the cosmic-ray exposure (CRE) ages of

\* Corresponding author. Fax: +1 (303) 546 9687.

E-mail address: [davidn@boulder.swri.edu](mailto:davidn@boulder.swri.edu) (D. Nesvorný).

meteorites. CRE ages measure the time interval spent in space between the meteoroid's formation as a diameter  $D < 3$  m body (following removal from a shielded location within a larger object) and its arrival at Earth. The CRE ages of most stony meteorites that have been recently accreted by the Earth and collected on its surface (hereafter recent meteorites) are between  $\sim 10$  and 100 Myr (e.g., Caffee et al., 1988; Marti and Graf, 1992; Graf and Marti, 1994; Welten et al., 1997). Because step (3) described above generally takes  $\ll 10$  Myr, the relatively long CRE ages of recent stony meteorites show that most must be slowly delivered to resonances via step (2).

One specific problem that we address in this paper is the origin of ordinary  $L$ -chondrite meteorites. The  $L$  chondrites are the most common group of meteorites in our collections with a relative fall frequency of 38% (Sears and Dodd, 1988; Keil et al., 1994). Many  $L$  chondrites were heavily shocked and degassed with  $^{39}\text{Ar}$ - $^{40}\text{Ar}$  ages around 500 Myr (e.g., Heymann, 1967; Turner, 1969, 1988; Bogard et al., 1976; Bogard, 1995; Keil et al., 1994). Based on these results, it has been suggested that the  $L$ -chondrite parent body suffered a major impact at  $\sim 500$  Ma (e.g., Haack et al., 1996). A more accurate  $^{39}\text{Ar}$ - $^{40}\text{Ar}$  dating has been recently reported on five selected  $L$ -chondrite meteorites (Korochantseva et al., 2006). These new results indicate that the impact occurred more precisely at  $470 \pm 5$  Ma.

Moreover, it was inferred from thermal histories of impact-heated rocks after the  $\approx 470$  Ma event (e.g., Smith and Goldstein, 1977; Bogard, 1995) and from the abundance of heavily shocked  $L$  chondrites that the parent body was catastrophically disrupted. The measured slow-cooling rates require that the original parent body had  $D \gtrsim 100$  km (see Haack et al., 1996, and references therein). These results hint on the orbital location of the  $L$ -chondrite parent body.

Breakups of  $D \gtrsim 100$  km objects in the main belt leave behind traces in the orbital distribution of asteroids in the form of prominent asteroid families (Hirayama, 1918). The number of known asteroid families suggest that  $\sim 20$   $D \gtrsim 100$  km asteroids disrupted in the past 3.5 Gyr (Nesvorný et al., 2005, 2006a; Durda et al., 2006). Most of these families are older than 1 Gyr (e.g., Vokrouhlický et al., 2006a) and/or have a taxonomic classification (Bus and Binzel, 2002; Cellino et al., 2002; Mothé-Diniz et al., 2005) that is incompatible with  $L$  chondrites (e.g., the Hygiea, Eunomia, Themis, Koronis, Maria, Eos, Vesta, and Nysa/Polana families).

Among the remaining families, the Flora family is the most plausible source for  $L$  chondrites for the following reasons: (i) the Flora family is located in the inner main belt ( $a = 2.2\text{--}2.35$  AU), very close to the  $v_6$  resonance, which is known to produce Earth-crossing objects with high Earth-impact probabilities (Gladman et al., 1997); (ii) the Flora family was produced by the catastrophic breakup of a  $\approx 200$ -km-diameter object (Durda et al., 2006), thus satisfying the constraints discussed above; (iii) studies of orbital dynamics suggest that the Flora family may have formed  $\sim 500$  Myr ago (Nesvorný et al., 2002a), which nicely corresponds to the time when  $L$  chondrites were heavily shocked; and (iv) Asteroid (8) Flora has an SIV (or SIII) type according to the classification of Gaffey

(1984). SIV-type asteroids are good compositional analogs for  $L$ -chondrite meteorites (see also Gaffey et al., 1993).

The results of Schmitz et al. (1996, 1997, 2001, 2003) and Schmitz and Häggström (2006) provide additional evidence that may link the  $L$  chondrites to the Flora family. These researchers found abundant fossil  $L$ -chondrite meteorites and iridium enrichment in a  $\approx 470$  Myr old marine limestone quarry in southern Sweden. They proposed that the terrestrial accretion rates of meteorites and IDPs at  $\approx 470$  Ma were at least one order of magnitude larger than at present. The perfect agreement between the terrestrial ages of fossil meteorites and the shock ages of recent  $L$ -chondrite meteorites shows that these meteorite groups must be linked to a single source (Korochantseva et al., 2006).

It is plausible that the arrival rate of meteorites on Earth increased suddenly after the formation of the Flora family because: (i) the population of near-Earth objects (NEOs) increased by a factor of several when an estimated  $\sim 10\%$  of Flora fragments could have been injected into the  $v_6$  resonance in the aftermath of the breakup (Zappalà et al., 1998; Nesvorný et al., 2002a); and (ii) the Earth-impact probability of objects evolving from the  $v_6$  resonance is  $\sim 1\text{--}2\%$ , a factor of several larger than the mean impact probability of NEOs (Gladman et al., 1997; Zappalà et al., 1998; Bottke et al., 2002). The iridium enrichment can be explained by a strong enhancement in the terrestrial accretion rate of cosmic dust, which is also naturally produced by the breakup of a large asteroid at the location of the Flora family. Indeed, Farley et al. (2006) showed that family-forming events can produce enhanced terrestrial accretion rate of dust lasting  $\gtrsim 1$  Myr.

Our baseline hypothesis in this paper is that the fossil meteorites found in Sweden were transported to Earth in the immediate aftermath of the Flora-family-forming event. Unlike the stony meteorites found today which have 10–100 Myr CRE ages, the Swedish fossil meteorites have CRE ages ranging between 0.1 and 1.5 Myr (Heck et al., 2004). This indicates that relatively little time elapsed from the moment these fragments were released in space and their impacts on Earth. Because the transport of material to resonances by the Yarkovsky effect occurs over longer time scales, we infer that these fragments must have been injected *directly* into a powerful main-belt resonance and then evolved to Earth-crossing orbits by gravitational perturbations from the planets (via step (3) described above).

To quantify these issues, we model here the transport of meteoroids from the Flora family to Earth. Motivated by the short CRE ages of the fossil meteorites, we limit our modeling effort to the early stages of delivery. Our model is described in Section 2. We use the model to determine: (i) the terrestrial accretion rate of meteorites from the Flora family within the first 2 Myr of its formation, and (ii) the CRE ages of meteorites delivered to the Earth at different times (Section 3). We compare these results to the available constraints in Section 4. For example, Heck et al. (2004) found that the fossil  $L$ -chondrite meteorites (Schmitz et al., 1997) with the shortest CRE ages ( $\approx 100$  kyr) impacted on the Earth  $\sim 1.5$  Myr earlier than the collected fossil meteorites with the longest ( $\approx 1.5$  Myr) CRE ages. With our model, we have been able to determine that the

first generation of meteoroids transported from the Flora region  $\approx 470$  Myr ago show comparably short CRE ages that correlate with their impact times on Earth.

## 2. Model

We model meteorite transport in two steps. In the first step, we populate a large number of orbits between 1.8 and 2.2 AU by test particles. We follow these test particles for 2 Myr, recording their orbital histories and whether they impact any of the terrestrial planets. This part of the model does not include information about the location of the breakup nor the ejection velocities of the fragments. It is simply used to sample a large number of orbits in the neighborhood of the Flora family and track them as they evolve by planetary perturbations. We neglect secondary breakups of fragments because the estimated collisional lifetimes of 0.1–1-m-sized meteoroids ( $\approx 5$ –10 Myr; Bottke et al., 2005b) greatly exceed the measured CRE ages of the fossil meteorites (0.1–1.5 Myr; Heck et al., 2004). We also neglect the effects of the Yarkovsky thermal drag (e.g., Bottke et al., 2006) because 0.1–1-m-sized meteoroids only drift  $0.5$ – $5 \times 10^{-3}$  AU over 1 Myr. Such a small semimajor axis change is insignificant in the context of this work.

In the second step, we select three orbital elements of the reference orbit (semimajor axis  $a$ , eccentricity  $e$ , and inclination  $i$ ) and assume that meteoroids have been ejected from the reference orbit with velocities  $\delta \hat{V} = (V_r, V_t, V_z)$ , where  $V_r$ ,  $V_t$ , and  $V_z$  are the radial, along-the-track and  $z$ -axis components of  $\delta \hat{V}$ , respectively. In our model, the reference orbit is a proxy for the actual (but unknown) orbit of the disrupted object immediately prior to its disruption. See Section 3.2 for our different choices of the reference orbit.

Our model for the ejection of small fragments has therefore the following parameters: (i) true anomaly,  $f$ , and argument of perihelion,  $\omega$ , of the parent body at the moment of breakup; and (ii)  $\delta \hat{V}$  of individual fragments. We discuss different assumptions for  $\delta \hat{V}$  below. We use the Gauss equations (Brouwer and Clemence, 1961; Bertotti et al., 2003) to calculate the orbits of individual fragments from their  $\delta \hat{V}$ .

Finally, we put together steps one and two. For each individual fragment produced in step two, we find its nearest neighbor among the test orbits tracked in step one (see Section 3.2 for a detailed description of the algorithm based on similarity of orbital elements). We then assume that the fragment's orbit has an orbital history identical to that of the test orbit. For each selected breakup scenario, we use model results to identify the main resonances responsible for the transfer of the ejecta to Earth-crossing space, determine the impact rate of the fragments on Earth as a function of time, and compare these results with constraints implied by the studies of fossil meteorites (Sections 3 and 4).

To integrate the test orbits we used a numerical code called SWIFT-RMVS3 (Levison and Duncan, 1994). The SWIFT-RMVS3 code is a symplectic, state-of-the-art  $N$ -body code that uses highly efficient and robust methods to track the evolution of planets and test bodies (Wisdom and Holman, 1991). Any impacts on Earth during the integration are explicitly recorded

by this code. To obtain the best-possible impact statistics at any time epoch, we used an Öpik-algorithm-based code (Öpik, 1951) which calculates the impact probabilities by randomizing the orbital longitudes of Earth and particles (Wetherill, 1967; Bottke et al., 1994). Specifically, we used the original code developed in Wetherill (1967) and adopted it to our application. The semimajor axes, eccentricities and inclinations of Earth and particles, which are used as input in the Wetherill code, were taken from the output of SWIFT-RMVS3 at  $10^4$ -yr intervals. Our runs included 7 planets (Venus to Neptune). We used a 15-day integration timestep.

## 3. Results

### 3.1. Preliminary analysis of the orbit transfer

We first describe results from three model cases with 200,000 test particles each. These results involve step-one modeling and disregard effects of the actual ejection velocity field produced by the breakup. Several specific disruption scenarios involving the step-two modeling will be discussed in the next section.

The test jobs described in this section were used to: (i) determine the effects of planetary configuration at the time of breakup on meteorite fall statistics; (ii) identify the main pathways of fast and efficient transfer of objects from the Flora region to Earth; and (iii) help to select initial orbits for our large simulation which tracked orbits of 1.2 million test particles over 2 Myr (see Section 3.2). This large number of test particles was needed to obtain satisfactory fall statistics for specific breakup scenarios.

The three small simulations described here used three different planetary epochs: the current epoch (E0 job), epoch 25,000 yr in the future (E25ky job) and another epoch 50,000 yr in the future (E50ky job). These epochs were selected to roughly span over one full rotational cycle of secular orbital angles. Our CPU limitations prevented us from using additional starting epochs. For each job, 200,000 test particles were randomly distributed in an orbital box with  $1.8 < a < 2.2$  AU,  $0.15 < e < 0.35$ , and  $i < 10^\circ$ . We did not sample orbits with  $a > 2.2$  AU because test bodies on these orbits are stable over Myr-long time scales and typically do not evolve to planet-crossing space over the time spans considered here (Morbidelli and Nesvorný, 1999). We did not sample orbits with  $a < 1.8$  AU because the ejection of fragments from the Flora region ( $a = 2.2$ – $2.35$  AU) onto these orbits would require ejection speeds in excess of  $2 \text{ km s}^{-1}$ . According to what we know about physics of large-scale impacts, it is unlikely that ejection speeds in excess of  $2 \text{ km s}^{-1}$  have occurred. The nodal longitude,  $\Omega$ , perihelion longitude,  $\varpi$ , and mean anomaly,  $M$ , of particles were selected randomly between  $0^\circ$  and  $360^\circ$ .

Fig. 1 shows the orbits of test particles used in the E0 job that were accreted by the Earth within the first 1 Myr after the start of the integration. In total, 210 out of initial 200,000 test particles (i.e., about 0.1%) impacted Earth within the first 1 Myr. Most of these particles evolved onto Earth-crossing orbits by the effect of secular resonance  $v_6$  located between 2.0

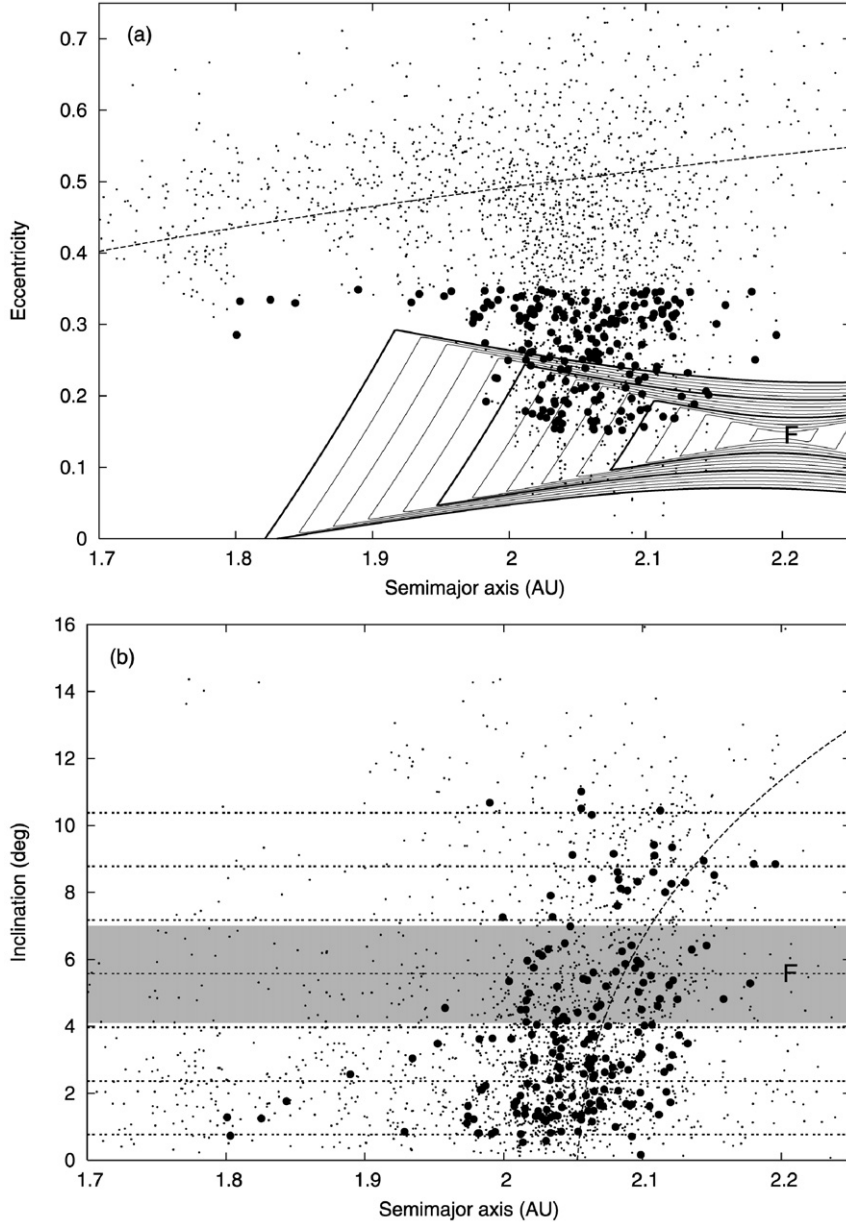


Fig. 1. Orbits of early impactors in the E0 simulation. The bold dots show the initial orbits of test particles that impacted on the Earth within the first 1 Myr. Small dots show how these orbits evolved. Letter 'F' denotes the orbit of (8) Flora. The solid contours in (a) show isolines of  $\sqrt{V_t^2 + V_r^2}$  values spaced by  $100 \text{ m s}^{-1}$ . The horizontal contours (b) show isolines of  $V_z$  spaced by  $500 \text{ m s}^{-1}$ . To define these isolines, we selected specific values of the true anomaly,  $f$ , and perihelion argument,  $\omega$ , of the parent body to maximize the orbital change with given  $V_t$ ,  $V_r$ ,  $V_z$ . The shaded area in (b) shows the range of  $i$  visited by (8) Flora at different times. Orbit above the dashed line in (a) are Earth-crossing. The dashed curved line in (b) shows the center of the  $v_6$  resonance for  $e = 0.1$ . The take-away message from these plots is that most early impactors on the Earth start with orbits separated from (8) Flora by  $\gtrsim 500 \text{ m s}^{-1}$ .

and 2.15 AU (e.g., Morbidelli and Henrard, 1991). These resonant orbits typically start evolving along the guiding trajectories in phase portraits of the  $v_6$  resonance determined by Morbidelli and Henrard (1991) until their  $e$  becomes large. The early impactors identified in our simulations are accreted on Earth almost immediately after their perihelion drops below 1 AU. Therefore, we identify the  $v_6$  resonance as the most important fast and efficient pathway from the Flora region to the Earth.

To inject fragments from Asteroid (8) Flora's orbit ( $a = 2.201 \text{ AU}$ ,  $e = 0.144$ , and  $i = 5.34^\circ$ ; Milani and Knežević, 1994) deep into the  $v_6$  resonance, the required ejection speeds

are  $\gtrsim 500 \text{ m s}^{-1}$  (Fig. 1). This is a high value compared to typically  $\lesssim 100 \text{ m s}^{-1}$  ejection speeds derived from studies of asteroid families for kilometer-sized and larger fragments produced by asteroid collisions (e.g., Michel et al., 2001, 2002; Bottke et al., 2001; Nesvorný et al., 2002b, 2006b; Vokrouhlický et al., 2006a, 2006b). Here, however, we deal with much smaller, typically meter-sized or smaller meteoroids. It has been noted in laboratory and hydrocode experiments that the typical speeds of fragments produced by a disruptive collision increase with their decreasing size (Nakamura, 1993; Michel et al., 2001, 2002). Therefore, ejection speeds of  $\sim 500 \text{ m s}^{-1}$  for meteoroid-sized

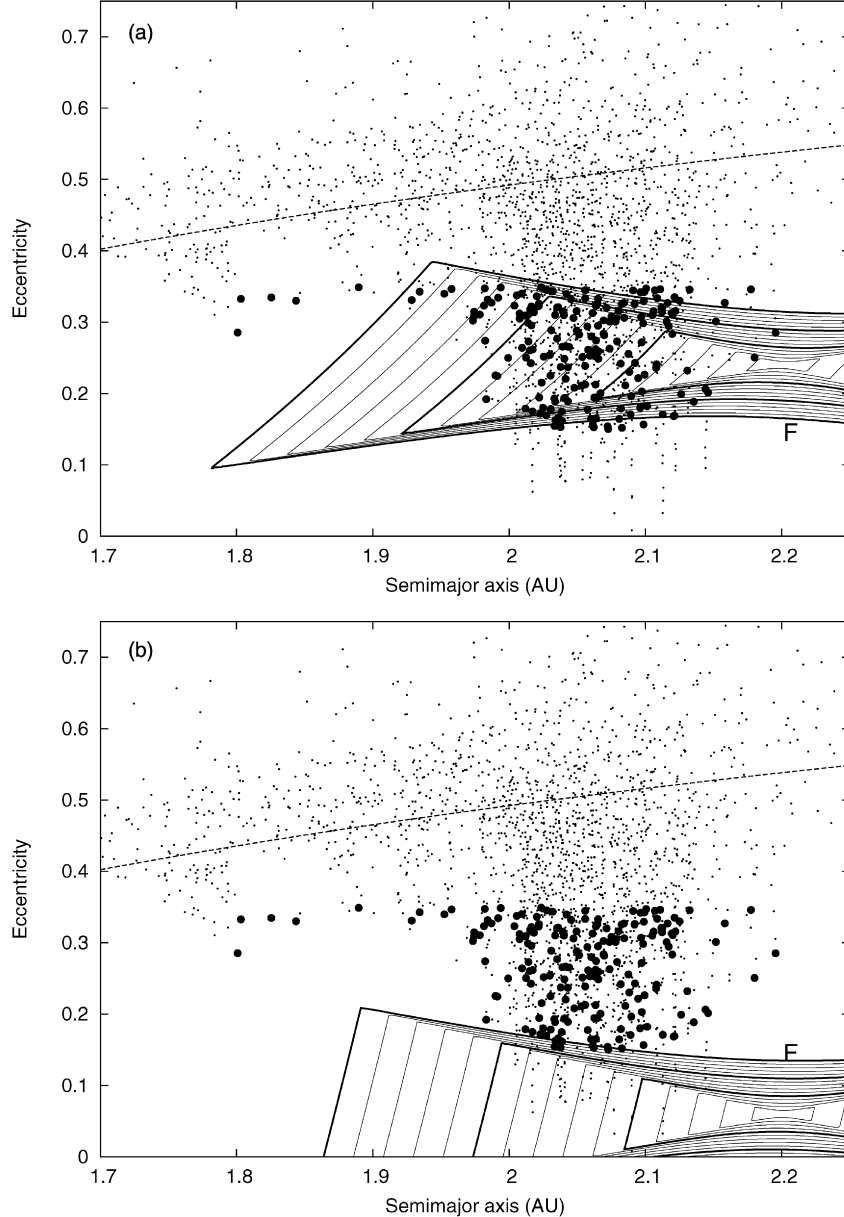


Fig. 2. The same as Fig. 1a but for the case where the ejection speed contours are centered at the maximal (upper panel) and minimal value (bottom panel) of  $e$  visited by (8) Flora during its orbital oscillations induced by the planets. For reference, letter ‘F’ denotes the mean  $(a, e)$  location of (8) Flora. In (a), a large fraction of fragments ejected with  $\delta V < 1 \text{ km s}^{-1}$  would impact on the Earth within the first 1 Myr after the breakup. In (b), the interesting orbits of fragments with small  $e$  were not sampled in the E0 simulation (we used  $e > 0.15$ ; Section 3.1).

fragments may be reasonable. Unfortunately, laboratory shot experiments and hydrocode simulation of asteroid impacts are done for unsuitably small impact energies and lack the necessary resolution, respectively, to properly determine the ejection speeds of meteoroid-sized fragments. For these reasons, we will assume here that speeds  $\gtrsim 500 \text{ m s}^{-1}$  may have occurred.

We found that the number of fragments injected from the Flora region into the  $v_6$  resonance depends sensitively on the *instantaneous* (osculating)  $e$  of the parent body at the moment of breakup. The osculating orbit of (8) Flora oscillates due to planetary perturbations (particularly because of the nearby  $v_6$  resonance) with  $e$  changing from 0.06 to 0.24; the parent body’s orbit probably experienced similar oscillations. The distribution

of ejecta produced by the disruption of the parent body then depends on whether its  $e$  was low or high at the time of the breakup. In the later case, a relatively large number of fragments ejected with speeds  $\gtrsim 500 \text{ m s}^{-1}$  end up deep in the  $v_6$  resonance and are quickly accreted by the Earth (Fig. 2). Therefore, a favorable phase of parent’s body eccentricity at the time of breakup could have increased the influx of early impactors reaching Earth.

Fig. 3 shows the number of impacts (per 50 kyr) recorded in the first 1 Myr in the E0, E25ky, and E50ky simulations. We used two complementary methods to calculate the fall statistics: (1) the number of impacts was recorded directly by the SWIFT-RMVS3 code; and (2) the impact probabilities were calcu-

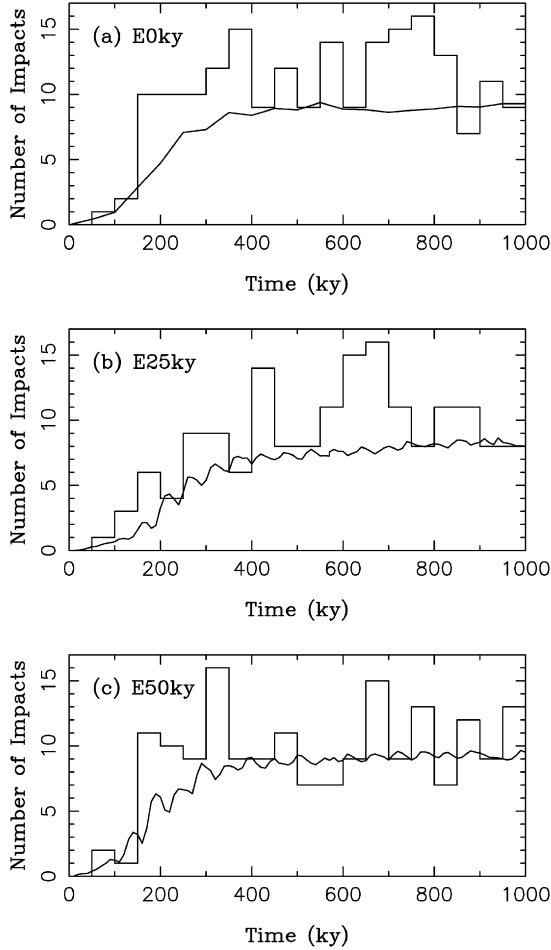


Fig. 3. The fall statistics from our E0 (a), E25ky (b), and E50ky (c) simulations. The number of impacts per 50-kyr interval is shown. The histograms outlined by the solid lines show impacts of individual test particles on the Earth as recorded by the SWIFT-RMVS3 code. The wavy solid lines show the fall statistics that were determined using an Öpik-algorithm-based code developed in Wetherill (1967). The sampling of output of the SWIFT-RMVS3 code was 50 kyr in E0 and 10 kyr in E25ky and E50ky. Therefore, the impact profiles calculated from the Wetherill code have finer sampling in (b) and (c) than in (a), and better reveal the real fluctuations of the impact rate. (It would be computationally expensive (and not really useful) to repeat the E0 integrations with a finer sampling.)

lated by an Öpik-algorithm-based code developed by Wetherill (1967). In (2), the orbits of the Earth and test particles were first recorded with constant sampling by SWIFT-RMVS3. This orbit information was then used in the Wetherill code to calculate collision probabilities and impact velocities between the Earth and each individual test particle. Method (2) assumes that nodal, perihelion and mean longitudes of test particles' orbits are distributed with uniform probability between  $0^\circ$  and  $360^\circ$ . The overall collisional probability determined from the Wetherill code was scaled to 200,000 objects in Fig. 3.

Method (1) is more precise than (2) because it uses more detailed orbit information than (2), but its use is limited due to small number statistics. Methods (1) and (2) agree to within a factor of two in Fig. 3. While part of the residual difference may be explained by small number statistics in (1), it seems that the overall number of impacts determined in (1) is systemati-

cally higher (by  $\approx 30\%$ ) than that found in (2), especially during the initial phase. Method (2) is known to underestimate impact rates in cases similar to the one described here where tangential orbits are common (Dones et al., 1999).

In general, the number of recorded impacts increased over the first 500-kyr and remained nearly constant over the second 500-kyr period (Fig. 3). Few impacts occurred in the first 150 kyr. These very early impacts are rare because the  $v_6$  resonance needs some minimal time, typically  $\gtrsim 150$  kyr, to increase  $e$  and produce Earth-crossing orbits.

Fig. 3 also shows that the detailed fall statistics depend on the phase of planetary orbits at the moment of breakup. In E0 and E50ky, the number of impacts increases more abruptly, in both cases around 150 kyr, than in E25ky. In E25ky, the number of recorded impacts steadily increases with time during the first 500 kyr. Also, the number of impacts in the E25ky job is about 30% lower within the first 500 kyr than that recorded in the E0 and E50ky jobs. We believe that the origin of these differences can be traced to the phase of the Earth's eccentricity at the time of the breakup and/or to the varying efficiency of the  $v_6$  resonance to deliver orbits to high  $e$  within short time spans.

The overall differences in fall statistics between jobs started at different epochs are not exceedingly large. The total number of impacts in 1 Myr registered in the E0, E25ky, and E50ky simulations only differ by 15%. This uncertainty does not affect our conclusions in Section 4. Larger uncertainties will be introduced into the final estimates by the unknown ejection speeds of meteoroid-sized fragments, the total number of fragments produced by the Flora family breakup, and the ablation effects on meteorites in the Earth's atmosphere. We deal with the first of these three issues in the next section.

### 3.2. Fall statistics for isotropic ejection velocities

The results described above helped us to determine the initial orbits for our large simulation, which used 1.2 million test particles distributed among 48 processors of the LeVerrier Beowulf computer cluster based at the Department of Physics and Astronomy of the University of British Columbia. Most of the Beowulf processors are Athlon 2600-MP CPUs. The orbit integration runs consumed approximately 2 months of CPU time on each processor. The purpose of this simulation was to obtain detailed Earth-impact statistics of a large number of initial test orbits. The meteoroids ejected from the Flora region may have sampled these orbits in different ways depending on our assumptions about their ejection velocities (see below).

The initial orbits of test particles were selected in a box with  $1.95 < a < 2.2$  AU,  $e < 0.35$  and  $i < 10^\circ$ . These orbits populated the same range of orbit parameters as those used in the small jobs from Section 3.1 except: (i) we sampled orbits with  $e < 0.15$  that would be populated by fragments in the case where the parent object disrupted near the minimum of its secular oscillations in  $e$  (Fig. 2b); (ii) we did not sample orbits with  $1.8 < a < 1.95$  AU because these orbits showed very few early impacts in our small jobs (Fig. 1). Angles  $\Omega$ ,  $\varpi$ , and  $M$  were selected randomly between  $0^\circ$  and  $360^\circ$ . Seven planets (Venus to Neptune) were included in the integration; their

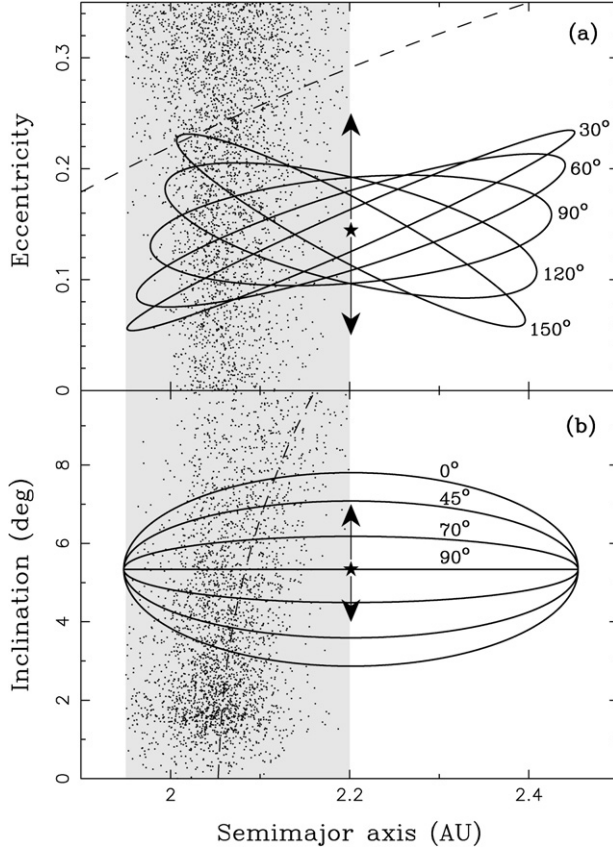


Fig. 4. The ellipses show the orbital locations of test particles launched from the current orbit (8) Flora (denoted by a star) with ejection speeds of  $1 \text{ km s}^{-1}$ . Different ellipses correspond to different choices of  $f$  and  $\omega$  in the Gauss equations. In (a), the labels denote different values of  $f$ . In (b), the labels denote values of  $f + \omega$ . The arrows show the range of secular oscillations of (8) Flora's orbit in  $e$  and  $i$ . The shaded area was sampled by our 1.2 million test orbits. The dots in the shaded area denote the initial orbits of 2944 test particles that impacted on the Earth in the first 2 Myr. Orbits above the dashed line in (a) are Mars-crossing. The center of the  $v_6$  resonance for  $e = 0.1$  is denoted by the dashed line in (b).

starting orbits were identical to those used in job E0. All orbits were integrated for 2 Myr with a 15-day integration timestep. The number of impacts and their timing was determined from the Wetherill collisional code. The number of direct impacts registered by the SWIFT-RMVS3 code was typically not large enough to provide useful statistics for specific ejection scenarios.<sup>1</sup>

The results were used in the following way. We generated  $10^5$  test bodies to represent a sample of meteoroid-sized fragments produced by the Flora breakup. To set up their orbits, we assumed that the fragments were ejected isotropically from the orbit location of the parent body defined by the orbital ele-

ments  $a_{\text{pb}}$ ,  $e_{\text{pb}}$ ,  $i_{\text{pb}}$ ,  $\Omega_{\text{pb}}$ ,  $\omega_{\text{pb}}$ , and  $f_{\text{pb}}$ . We used the current orbit of (8) Flora, the largest object in the Flora family, as a proxy for the parent body's orbit. We used the isotropic ejection velocities of fragments as a simple and plausible parametrization of the velocity field. Anisotropic velocities may lead to larger or smaller impact rates depending on the orientation of the mean velocity vector of fragments, which may or may not favor injection of orbits into the  $v_6$  resonance. Studying the effects of anisotropy is beyond the scope of this paper.

The ejection velocity vectors of individual fragments,  $\delta \hat{V} = (V_r, V_t, V_z)$ , were chosen to represent the Gaussian distribution in each velocity component with variance  $\sigma$ . With this choice, the magnitude of the ejection velocities is distributed according to the Maxwellian distribution with mean speed  $\langle \delta V \rangle = 2\sigma\sqrt{2/\pi} \approx 1.6\sigma$ . Once  $\delta \hat{V}$  of individual fragments were selected the initial orbital elements were determined from the Gauss equations (Brouwer and Clemence, 1961; Bertotti et al., 2003), where we used  $f = f_{\text{pb}}$  and  $\omega = \omega_{\text{pb}}$  to set up the orbital phase of breakup. Fig. 4 illustrates the ejection velocity field for  $\delta V = 1 \text{ km s}^{-1}$  and different choices of  $f$  and  $\omega$ .

Taken together, there are 7 parameters that define the initial orbits of our synthetic Flora meteoroids:  $\langle \delta V \rangle$ ,  $a_{\text{pb}}$ ,  $e_{\text{pb}}$ ,  $i_{\text{pb}}$ ,  $\Omega_{\text{pb}}$ ,  $\omega_{\text{pb}}$ ,  $f_{\text{pb}}$ . We vary these parameters to determine their effect on the number of impacts on the Earth. First, the orbit of each synthetic meteoroid is compared with the initial orbits of 1.2 million test particles that we tracked in our large simulation. The impact history of each synthetic meteoroid is then set to correspond to the pre-determined impact histories of its neighbor test orbits. Specifically, we use all test orbits that fall within the neighborhood cell with dimensions 0.005 AU, 0.01, and  $0.2^\circ$  in  $a$ ,  $e$ , and  $i$ . The large number of tracked test orbits means that cells contain on average 14 test orbits.

The effect of  $\Omega_{\text{pb}}$ ,  $\omega_{\text{pb}}$ , and  $f_{\text{pb}}$  on impact statistics is twofold: (1) Angles  $\omega_{\text{pb}}$  and  $f_{\text{pb}}$  enter the Gauss equations and determine the shape of the region in orbital space that becomes populated by fragments (Fig. 4). (2) Angles  $\Omega_{\text{pb}}$  and  $\omega_{\text{pb}}$  determine the starting phase of secular evolution for each orbit.

To test (2), we analyzed the initial  $\Omega$  and  $\omega$  of test orbits that showed impacts on the Earth. In total, the SWIFT-RMVS3 code recorded 2944 impacts on the Earth in 2 Myr; i.e., about 2.5 impacts for every 1000 test bodies (Fig. 5). We found that the distributions of initial  $\Omega$ ,  $\omega$  and  $\varpi = \Omega + \omega$  of these orbits were nearly uniform. Therefore, the overall impact statistics cannot be overly sensitive to (2). This result helps us to justify the procedure described above where we use cells in  $a$ ,  $e$ , and  $i$ , and do not resolve their dependence on  $\Omega$  and  $\omega$ . In the following we determine the overall impact statistics as a function of  $\langle \delta V \rangle$ ,  $a_{\text{pb}}$ ,  $e_{\text{pb}}$ ,  $i_{\text{pb}}$ ,  $\omega_{\text{pb}}$ , and  $f_{\text{pb}}$ , where  $\omega_{\text{pb}}$  and  $f_{\text{pb}}$  enter via (1). (We will analyze effect (2) later in this section.)

Fig. 6 shows the fraction of synthetic meteoroids that impacted the Earth in the first 0.5, 1, and 2 Myr. We denote these fractions  $F_{0.5 \text{ Myr}}$ ,  $F_{1 \text{ Myr}}$ , and  $F_{2 \text{ Myr}}$ , respectively. In three different tests, we launched meteoroids using three different values of  $e_{\text{pb}}$  to test the dependence of impact rate on  $e_{\text{pb}}$ . These tests showed that more impacts occurred for  $e_{\text{pb}} = 0.25$  than for smaller values of  $e_{\text{pb}}$ , possibly because the larger starting ec-

<sup>1</sup> This becomes clear when the total number of registered direct impacts ( $N = 2944$ ; see below) is compared with the number of orbital cells needed to obtain a satisfactory resolution in orbital-element space ( $N_{\text{cell}} = 87,500$ ; see below). Because  $N_{\text{dimp}} \ll N_{\text{cell}}$ , the impact statistics cannot be inferred from direct impacts for most cells. It then becomes problematic to use the registered direct impacts as a reliable measure of the impact rate. The direct impact statistics is further diluted when we attempt to resolve the impact rate as a function of time.

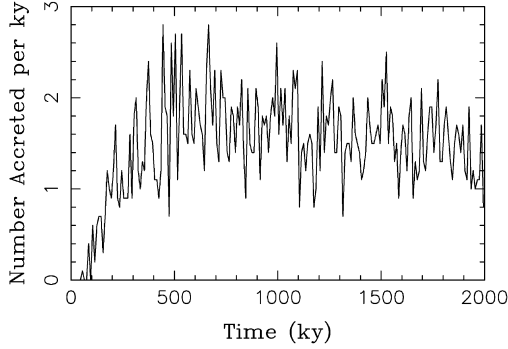


Fig. 5. The number of direct impacts on the Earth as recorded by the SWIFT-RMVS3 code. In total, 1.2 million test particles were distributed in orbits according to the procedure described in the main text. The test particles were followed over 2 Myr or until they hit the Sun or a planet. This plot shows how the recorded number of impacts on the Earth changes with time. The profile was smoothed by a moving 10-kyr window. The impact rate steeply raises over the first 500 kyr and then it slowly declines over a much longer timescale. In total, the SWIFT-RMVS3 code recorded 2944 impacts on the Earth in 2 Myr (out of 1.2 million launched particles). Note that this figure shows the impact rate for the entire grid of initial conditions and does not take into account a realistic ejection velocity field.

centricities favor earlier transport times via  $v_6$  to Earth-crossing orbits.

The number of impacts is a steadily increasing function of  $\langle \delta V \rangle$  in Fig. 6. Values of  $\langle \delta V \rangle$  in excess of  $400 \text{ m s}^{-1}$  are apparently needed to produce  $F_{1 \text{ Myr}} > 10^{-4}$ . For  $\langle \delta V \rangle = 500 \text{ m s}^{-1}$ ,  $F_{1 \text{ Myr}}$  ranges between  $1.4 \times 10^{-4}$  for  $e_{\text{pb}} = 0.05$  to  $2.6 \times 10^{-4}$  for  $e_{\text{pb}} = 0.25$ . Impact statistics based on the number of impacts directly recorded by the SWIFT-RMVS3 code in our small jobs (see previous section) suggests that  $F_{1 \text{ Myr}}$  could be about 30% larger than these values. Unfortunately, the statistics based on direct impacts cannot be reliably inferred here for individual disruption scenarios. Therefore, we are not sure whether the values computed from Wetherill algorithm indeed underestimate the impact rate by 30% as hinted by the results obtained in the previous section.

$F_{0.5 \text{ Myr}}$  is more sensitive to the exact value of  $e_{\text{pb}}$  than  $F_{1 \text{ Myr}}$  and  $F_{2 \text{ Myr}}$ , showing that  $e_{\text{pb}}$  controls the total number of very early impacts. The ratio  $F_{0.5 \text{ Myr}}:F_{1 \text{ Myr}}:F_{2 \text{ Myr}}$  for  $e_{\text{pb}} = 0.15$  is about 1:4:10. Therefore, relatively more impacts occur at later times than immediately after the breakup. This result is not surprising because meteoroids must spend some time in the  $v_6$  resonance before they can be delivered onto Earth-crossing orbits.

Fractions  $F$  also sensitively depend on the value of  $a_{\text{pb}}$ . To illustrate this dependence, we plot  $F_{0.5 \text{ Myr}}$ ,  $F_{1 \text{ Myr}}$ , and  $F_{2 \text{ Myr}}$  for  $a_{\text{pb}} = 2.15$ , 2.2, and 2.25 AU in Fig. 7. These impact rates are large for  $a_{\text{pb}} = 2.15$  AU, even for relatively small values of  $\langle \delta V \rangle$ . For example,  $F_{1 \text{ Myr}} = 2 \times 10^{-4}$  for  $\langle \delta V \rangle = 200 \text{ m s}^{-1}$ . Fraction  $F_{1 \text{ Myr}}$  peaks near  $\langle \delta V \rangle = 600 \text{ m s}^{-1}$  for  $a_{\text{pb}} = 2.15$  AU. An orbit with  $a_{\text{pb}} = 2.15$  AU, however, is not located in a dynamically stable part of the main belt because it is too close to the  $v_6$  resonance. Therefore, it is unlikely that a breakup with  $a_{\text{pb}} = 2.15$  AU has actually occurred.

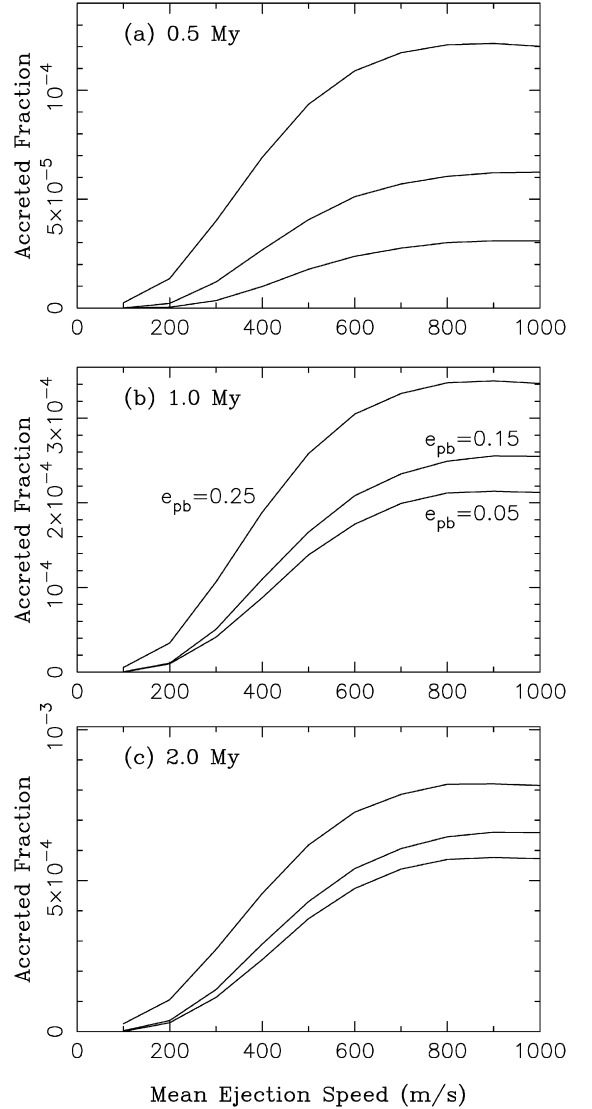


Fig. 6. The number fraction of synthetic meteoroids accreted on Earth within the first 0.5 Myr (a), 1 Myr (b), and 2 Myr (c). This result was obtained by using the Wetherill algorithm. The meteoroids were launched from  $a_{\text{pb}} = 2.202 \text{ AU}$  and  $i_{\text{pb}} = 5.9^\circ$  assuming  $f_{\text{pb}} = 90^\circ$  and  $f_{\text{pb}} + \omega_{\text{pb}} = 45^\circ$ . The solid lines show the result for three values of  $e_{\text{pb}}$  spanning the range of eccentricity oscillations of (8) Flora. From bottom to top, these values are  $e_{\text{pb}} = 0.05$ , 0.15, and 0.25. In all cases, the number of impacts is a steadily increasing function of  $\langle \delta V \rangle$  (shown on x-axis).

The Flora family extends from  $a = 2.18$  AU to  $a = 2.35$  AU. The largest object in the family,  $\approx 136$ -km-diameter Asteroid (8) Flora, is located near the inner semimajor axis edge of the family, at  $a \approx 2.2$  AU. If the semimajor axis of (8) Flora is a good proxy for  $a_{\text{pb}}$ , this would suggest that the parent body of the Flora family disrupted at an almost ideal orbital position near the  $v_6$  resonance. The expected impact rates from a breakup at such a location are plotted in Fig. 7. These rates are relatively large. For example,  $F_{2 \text{ Myr}} \approx 4 \times 10^{-4}$  for  $a_{\text{pb}} = 2.15$  AU and  $\langle \delta V \rangle = 500 \text{ m s}^{-1}$ .

With  $a_{\text{pb}} = 2.25$  AU, the parent body would be more centered in the Flora family than (8) Flora (see Nesvorný et al., 2002a). Fractions  $F$  are lower for this value of  $a_{\text{pb}}$  (Fig. 7) be-

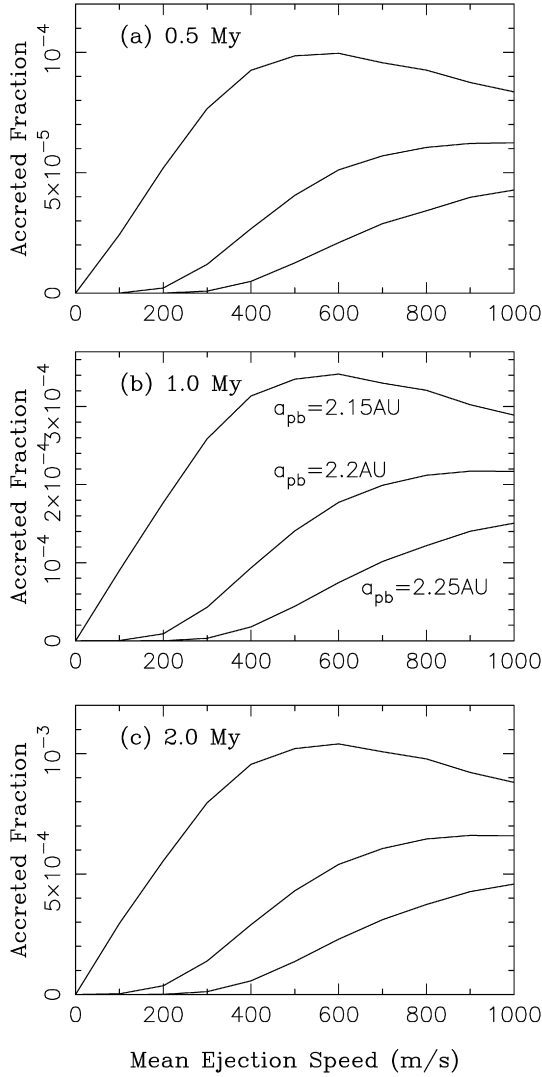


Fig. 7. The same as Fig. 6 but for meteoroids launched from  $e_{pb} = 0.15$  and  $i_{pb} = 5.9^\circ$  assuming  $f_{pb} = 90^\circ$  and  $f_{pb} + \omega_{pb} = 45^\circ$ . The solid lines show the result for  $a_{pb} = 2.15, 2.2$ , and  $2.25 \text{ AU}$ .

cause meteoroids need to be ejected with larger speeds to reach the  $v_6$  resonance location and to evolve to the Earth-crossing orbits shortly after the breakup.

The above results use uniformly random distributions of  $\varpi$  and  $\Omega$  of the ejected fragments. As such, these results illustrate averaged impact rates that do not depend on these angles. In reality, fragments ejected from the impact site will have a tight range of  $\varpi$  and  $\Omega$  within  $\sim 1^\circ$  or so about values defined by the osculating orbit of the parent body at the time of the breakup. In the Flora region, the eccentricity of an asteroid shows large oscillations in phase with  $\varpi - \varpi_6$ , where  $\varpi_6$  is one of the principal planetary frequencies (these oscillations are produced by the neighbor  $v_6$  resonance; Morbidelli and Henrard, 1991). The minimum of  $e$  occurs when  $\varpi - \varpi_6 = 0$  and the maximum of  $e$  occurs when  $\varpi - \varpi_6 = 180^\circ$ . Therefore, the exact value of  $\varpi - \varpi_6$  at the time of the breakup is important because it controls the mean value of  $e$  of the ejected fragments.

To account for the above effect, we have determined the impact rate statistics as a function of  $\varpi - \varpi_6$ . We assumed that the orbit of (8) Flora is a good proxy for the parent body's orbit. We have numerically integrated the orbit of (8) Flora with all relevant planetary perturbations included. Using the result of this numerical integration, we parametrized  $e$  as a function of  $\varpi - \varpi_6$ . The initial phase and frequency of  $\varpi_6$  were extracted from the output of the integration by a Fourier-based technique (Šídlichovský and Nesvorný, 1997). Specifically, we found that  $e \approx 0.15 - 0.05 \cos(\varpi - \varpi_6)$ .

We then fix  $e_{pb}$  and  $\varpi_{pb} - \varpi_6$  (where  $\varpi_{pb} = \Omega_{pb} + \omega_{pb}$ ) so that the above relationship holds and calculate impact rates with  $a_{pb} = 2.2 \text{ AU}$ ,  $i_{pb} = 5.9^\circ$  and various values of  $\delta V$  (Fig. 8). We parametrize different impact rate profiles by the initial value of  $\varpi_{pb} - \varpi_6$ . These results respect the secular orbit dynamics of the disrupted parent asteroid more accurately than the ones illustrated in Fig. 6.

Fig. 8 shows that the largest impact efficiencies occur for  $\varpi_{pb} - \varpi_6 \approx 135^\circ$  which corresponds to an intermediate value of  $e_{pb}$  ( $\approx 0.185$ ). Other phases of  $\varpi_{pb} - \varpi_6$  produce lower or larger initial values of  $e_{pb}$  but always lead to lower impact efficiencies of fragments. This result stems from the orbit dynamics of the  $v_6$  resonance which determines how fragments reach the Earth-crossing orbits. The phase portraits of the  $v_6$  resonance (Morbidelli and Henrard, 1991) serve as an important guide. These portraits show that the orbits started with  $\varpi - \varpi_6 \approx 135^\circ$  are transferred to high  $e$  faster than orbits with any other initial phase of  $\varpi - \varpi_6$ . Conversely, the orbits started with  $\varpi - \varpi_6 \approx 270^\circ$  require longest transfer times and lead the lowest impact efficiencies (bottom lines in Fig. 8).

The overall impact efficiencies in Fig. 8 are similar to those that we estimated with our previous ( $\varpi$ -averaged) model and showed in Fig. 6. In reality, the true impact efficiencies will be a combination of the results shown in Figs. 6 and 8 because the secular oscillations of  $e_{pb}$  in the Flora region include terms both correlated (as accounted for in Fig. 8) and uncorrelated with  $\varpi - \varpi_6$  (Fig. 6). It is difficult to present more deterministic results here due to unknown orbit of the parent body at the time of the breakup.

Additional tests (similar to those described above but where additional parameters of our model were varied) showed that the effect of other parameters of the ejection field, namely  $i_{pb}$ ,  $\Omega_{pb}$ ,  $\omega_{pb}$ , and  $f_{pb}$ , on the impact rate is small. As we discuss in the next section, however, the exact value of  $f_{pb}$  can have an important effect on the very early accretion history (within  $\approx 300$  kyr after breakup) of Flora meteoroids.

To summarize, we found that fraction  $F_1 \text{ Myr}$  is generally an increasing function of  $\langle \delta V \rangle$  with values typically  $1-3 \times 10^{-4}$  for  $\langle \delta V \rangle = 500 \text{ m s}^{-1}$ . For special choices of  $a_{pb}$  and  $e_{pb}$ ,  $F_1 \text{ Myr}$  for  $\langle \delta V \rangle = 500 \text{ m s}^{-1}$  may be as high as  $4 \times 10^{-4}$  or as low as  $5 \times 10^{-5}$ . Values of  $F_{0.5 \text{ Myr}}$  and  $F_{2 \text{ Myr}}$  show similar dependences but are typically 4 times smaller and 2.5 times larger, respectively, than  $F_1 \text{ Myr}$ . These estimates provide an important link between the number of meteoroid-sized fragments produced by the Flora breakup and the number (and mass) of recovered fossil meteorites.

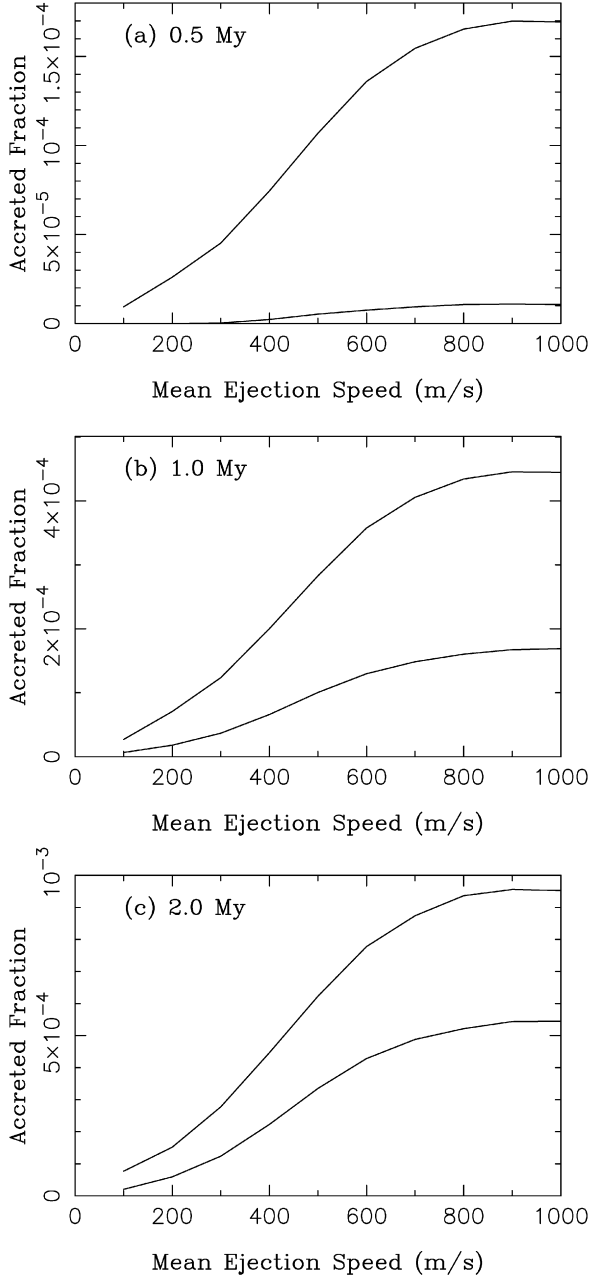


Fig. 8. The number fraction of synthetic meteoroids accreted on Earth within the first 0.5 My (a), 1 My (b), and 2 Myr (c). This result was obtained by using the Wetherill algorithm. The meteoroids were launched from  $a_{\text{pb}} = 2.2$  AU and  $i_{\text{pb}} = 5.9^\circ$  assuming  $f_{\text{pb}} = 90^\circ$  and  $f_{\text{pb}} + \omega_{\text{pb}} = 45^\circ$ . The solid lines show the result for two values of  $\omega_{\text{pb}} - \omega_6$ . These values have been selected to maximize (upper lines in each panel;  $\omega_{\text{pb}} - \omega_6 = 135^\circ$ ) and minimize (lower lines;  $\omega_{\text{pb}} - \omega_6 = 270^\circ$ ) the impact efficiencies. The number of impacts is a steadily increasing function of  $\langle \delta V \rangle$  (shown on x-axis) for  $\langle \delta V \rangle \lesssim 800$  m s $^{-1}$  and tends to be more constant for  $\langle \delta V \rangle \gtrsim 800$  m s $^{-1}$ .

#### 4. Discussion

We advocate here a model for the origin of fossil meteorites that has the following components: (i) the meteoroid-sized fragments are released from their parent body by the Flora-family breakup some 470 Myr ago; (ii) many of these fragments are injected into the  $\nu_6$  resonance; (iii) the meteoroids evolve to

Earth-crossing orbits as their orbital eccentricity gets pumped up by the  $\nu_6$  resonance; and (iv) a small fraction of meteoroids go on to strike Earth within 2 Myr after the breakup.

This model can be constrained by data. Specifically, we use the following three constraints: (1) It has been inferred from the fall statistics that the meteorite flux during the Ordovician was  $\sim 10$ –100 times higher than at present (Schmitz et al., 2001). This poses a severe constraint on the number of meteoroids produced by the breakup and on the efficiency of their accretion by the Earth. (2) The CRE ages of fossil meteorites are short (0.1–1.5 Myr) and appear to be correlated with depth in which they have been found in the quarry (Heck et al., 2004). This suggests that a large number of fragments must have been accreted by the Earth within a short time interval after the breakup event. (3) The abundance of fossil meteorites and their tracer elements (see below) found in different depths is broadly similar showing that the accretion rate did not change much in the first several Myr after the sharp start of the event.

To compare our model with constraints (2) and (3) we calculated the accretion rate of Flora meteorites on Earth as a function of time for different ejection velocity fields. As in the tests described in the previous section, it turns out also here that the accretion rate is mainly dependent on  $e_{\text{pb}}$  and  $\omega_{\text{pb}} - \omega_6$  ( $a_{\text{pb}}$  is kept constant here). Fig. 9 shows the result for two representative cases. As illustrated in this figure, the accreted fraction is small during the initial phase whose exact duration depends on model parameters. With a favorable choice of these parameters, the delay between the breakup and the onset of elevated impact rate can be as short as  $\approx 100$  kyr (as illustrated by upper line in Fig. 9). More typically, however, the delay is 200–400 kyr. Therefore, we would not expect from our model many fossil Flora meteorites with CRE ages shorter than  $\approx 200$ –400 kyr (unless special values of model parameters are assumed).

After this initial phase the number of accreted Flora meteorites sharply increases and eventually reaches a phase where the number of impacts is roughly constant or slowly decreases (with oscillations induced by secular dynamics<sup>2</sup>); typically  $2$ – $8 \times 10^{-7}$  kyr $^{-1}$  impacts occur during this latter phase (per one launched Flora meteoroid). Based on this result, we predict that the number of fossil meteorites in different depths of the sediment column could peak at 100–400 kyr after the breakup and should stay roughly equal for 300–500 kyr  $\lesssim t < 2$  Myr, where  $t$  is the time elapsed from the breakup. Therefore, the CRE ages  $\gtrsim 100$ –400 kyr should be common. These predictions nicely match the data obtained on fossil meteorites (Schmitz et al., 1996, 1997, 2001, 2003; Schmitz and Häggström, 2006; Heck et al., 2004).

Heck et al. (2004) found that some of the fossil meteorites collected in the lowermost Arkeologen bed show CRE ages  $\lesssim 100$  kyr. These extremely short CRE ages are difficult to pro-

<sup>2</sup> The waves of the accreted fraction have  $\approx 50$ -kyr periodicity. We believe that these waves (and those that appear in Fig. 3) are caused by oscillations of meteoroid's orbital eccentricity with a  $2\pi/g_6$  period, where  $g_6 = 28.25''/\text{yr}$  is one of the main planetary frequencies. Due to these oscillations, the perihelion distance of evolving orbits may be driven in and out of Earth-crossing space causing fluctuations in the impact rates.

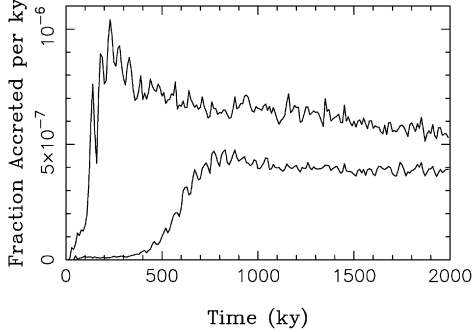


Fig. 9. The time-resolved fall statistics of Flora meteoroids that were launched with  $a_{\text{pb}} = 2.2$  AU,  $i_{\text{pb}} = 5.9^\circ$ , and  $f_{\text{pb}} + \omega_{\text{pb}} = 45^\circ$ . The upper line illustrates the result with  $\langle \delta V \rangle = 1 \text{ km s}^{-1}$ ,  $f_{\text{pb}} = 150^\circ$ ,  $\varpi_{\text{pb}} - \varpi_6 = 135^\circ$ , and  $e_{\text{pb}} = 0.25$ . These values were chosen to illustrate a case where the first impacts occur early ( $\approx 100$  kyr after the breakup) and the overall impact efficiency is large. The lower line corresponds to  $\langle \delta V \rangle = 500 \text{ m s}^{-1}$ ,  $f_{\text{pb}} = 90^\circ$ ,  $\varpi_{\text{pb}} - \varpi_6 = 270^\circ$ , and  $e_{\text{pb}} = 0.1$ . This latter case illustrates a breakup scenario with a long delay between the breakup and occurrence of first impacts on the Earth ( $\approx 500$  kyr), and low overall impact efficiency. Number of impacts per 1-kyr interval is shown. The plot can be interpreted as the distribution of CRE ages expected from our model.

duce in our model (Fig. 9) unless we use  $\langle \delta V \rangle \gtrsim 1 \text{ km s}^{-1}$  and/or very special configurations of the ejection velocity field (like those produced by small  $a_{\text{pb}}$  and/or  $e_{\text{pb}} \sim 0.25$  and  $f_{\text{pb}} \sim 180^\circ$  and/or special values of  $\varpi_{\text{pb}}$ ). Alternatively, Heck et al. (2004) may have underestimated the CRE ages of fossil meteorites by a factor of  $\sim 2$  possibly because of  $^{21}\text{Ne}$  loss by  $\sim 50\%$ . If such a large gas loss would have occurred we would expect a preferential loss of  $^3\text{He}$  (relative to  $^{21}\text{Ne}$ ) in meteorite Golvsten 001, which has been particularly well preserved. This contradicts measurements (Heck et al., 2004) and makes the  $\sim 50\%$  gas loss problematic. Further work will be needed to clarify this issue.<sup>3</sup>

As for constraint (1), Schmitz et al. (2001) estimated from the collected samples that the total mass of fossil meteorites over a horizontal area of  $6000 \text{ m}^2$  and a vertical sediment segment corresponding to a  $\approx 1.75$ -Myr time interval is  $\approx 10.4 \text{ kg}$ . By extrapolating this mass to the whole Earth surface, we estimate that the total mass accreted by the Earth within the  $\approx 1.75$ -Myr span was  $\sim 10^{12} \text{ kg}$ . This is an order of magnitude estimate. The error bar of this estimate, which can be very large, cannot be estimated unless we understand something about the variation of the fossil meteorite flux over the Earth surface. This

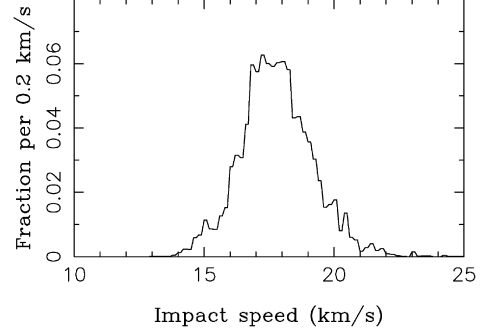


Fig. 10. The distribution of impact speeds of synthetic Flora meteoroids that accreted on the Earth in 1 Myr after the breakup. This result was obtained using the Wetherill code. The meteoroids were launched from  $a_{\text{pb}} = 2.202$  AU,  $e_{\text{pb}} = 0.15$ , and  $i_{\text{pb}} = 5.9^\circ$  assuming  $f_{\text{pb}} = 90^\circ$  and  $f_{\text{pb}} + \omega_{\text{pb}} = 45^\circ$ . The distributions of impact speeds obtained with different values of these parameters were similar to the one shown here. The distributions of impact speeds for all impacts in 0.5 and 2 Myr after the breakup are similar to the one obtained with the 1-Myr cutoff. All these distributions including the one plotted here are narrower than the ones determined for late impacts from the  $v_6$  resonance by Morbidelli and Gladman (1998).

will need more laboratory work.<sup>4</sup> Let  $f_{\text{abl}} < 1$  be the ablation factor that we define as the mass ratio between the meteorite fragments collected on the surface and the initial mass of their precursor meteoroid. Then,  $10^{12} f_{\text{abl}}^{-1} \text{ kg}$  is the inferred total mass of meteoroids in space.

From our simulations of the Flora meteoroids,  $F_{1.75 \text{ Myr}} \approx 2\text{--}6 \times 10^{-4}$  of fragments produced in the Flora region are accreted by the Earth within 1.75 Myr after the breakup (assuming  $\langle \delta V \rangle \sim 500 \text{ m s}^{-1}$ ). Therefore,  $1.5\text{--}5 \times 10^{15} f_{\text{abl}}^{-1} \text{ kg}$  is the total estimated mass of Flora meteoroids needed to reproduce the flux inferred from Schmitz et al. (2001).

Factor  $f_{\text{abl}}$  depends on many parameters including the pre-atmospheric speeds and entry angles of meteoroids. Using our model, we estimate that the pre-atmospheric speeds of Flora meteoroids were  $15\text{--}20 \text{ km s}^{-1}$  (Fig. 10; see also Morbidelli and Gladman, 1998). Borovička and Kalenda (2003) determined that  $f_{\text{abl}} = 0.2\text{--}0.05$  for six studied meteorite falls (see also Ceplecha and Revelle, 2005, and references therein). The pre-atmospheric speeds of these meteorite falls were estimated to be  $14.1\text{--}22.5 \text{ km s}^{-1}$ , nicely spanning the range determined for our synthetic Flora meteorites. We will assume  $f_{\text{abl}} = 0.2\text{--}0.05$  in the following calculations.

The parent body of the Flora family had diameter  $\approx 200 \text{ km}$  (Durda et al., 2006) and the corresponding mass  $\approx 10^{19} \text{ kg}$  (assuming bulk density  $\rho = 2700 \text{ kg m}^{-3}$ ). Let  $f_{\text{met}}$  be the fraction of this mass that was deposited into meteoroid-sized fragments. We then infer from the mass constraint that  $f_{\text{met}} = 1.5\text{--}5 \times 10^{-4} f_{\text{abl}}^{-1}$  or  $\approx 7.5\text{--}100 \times 10^{-4}$ .

The number of meteoroid-sized fragments produced by large asteroid collisions is unknown. Therefore, we can only compare the above derived value with simple parameterizations of

<sup>3</sup> Yet another possibility is that our model may inadequately ignore the effect of collisions. Immediately after the Flora family breakup the population of meteoroids in the inner main belt may have increased by a factor of  $\sim 100$ . If so, the collisional lifetime of these bodies may have become  $\sim 100$  times shorter than it is now. Extrapolating from the results of Bottke et al. (2005b), we estimate that the collisional lifetimes of 0.1–1-meter-sized meteoroids may have become  $\sim 50\text{--}100$  kyr in aftermath of the breakup matching the shortest CRE ages reported in Heck et al. (2004). If these short collisional ages indeed apply, however, it is not clear whether the impact rate of Flora meteoroids could have been sustained on nearly constant level over 1–2 Myr. Moreover, a collisional cascade would not produce CRE ages that are correlated with impact times (Heck et al., 2004) unless the collisional rates stayed initially elevated but dropped quickly after  $\sim 100$  kyr.

<sup>4</sup> Note that the global increase of the meteorite impact rate as the one advocated here should not produce strong fluctuations between different sites on the Earth surface. This can be verified by determining the fossil meteorite abundance at distant locations around the globe.

the size–frequency distribution (SFD) of fragments. For example, by assuming that the SFD of fragments produced by a breakup is steep for large (effective) diameters  $D$ , as suggested by the observed steep SFD of large asteroids in the Flora family (Morbidelli et al., 2003),  $N(D) \propto D^{-\alpha}$  where  $N(D)$  is the number of fragments with diameters between  $D$  and  $D + dD$  and  $\alpha \sim 5$  for  $D > 5$  km.

This steep SFD cannot continue to much smaller  $D$  because the total mass would be too large. Therefore, it is likely that the SFD slope becomes more shallow somewhere for  $D < 5$  km (Morbidelli et al., 2003). If we assumed that the SFD for  $D < 5$  km is the Dohnanyi distribution with  $\alpha = 3.5$  (Dohnanyi, 1969), we would find that the mass contained in  $D \sim 10$  cm fragments implies  $f_{\text{met}} \sim 4 \times 10^{-3}$ . This value of  $f_{\text{met}}$  is in the range of values derived above.<sup>5</sup>

Therefore, we find it plausible that the breakup of a  $D \approx 200$ -km asteroid at the orbital location of the Flora family may have produced a population of meteoroids large enough to match constraint (1) listed above. Together, our results show that all currently available constraints provided by studies of fossil meteorites can be satisfactorily matched in our model.

These results may also have important implications for the origin of recent  $L$ -chondrite meteorites. The link comes from the exact time correspondence between the age of fossil meteorites (Schmitz et al., 2001) and the shock ages of recent  $L$  chondrites (Korochantseva et al., 2006), both dated at  $\approx 470$  Ma. This correspondence strongly suggests that these two meteorite groups can be traced back to the same event. The results of Nesvorný et al. (2002a) and the ones presented here then link this event with the breakup of a  $\approx 200$ -km-diameter asteroid in the inner main belt that produced the Flora family.

Specifically, we believe that the recent  $L$ -chondrite meteorites may represent a tail of late impactors from the Flora family breakup (Nesvorný et al., 2002a). Morbidelli and Gladman (1998) have analyzed the long-term orbital evolution of objects started in the  $v_6$  resonance. Their results provide hints about the impact rate of Flora meteoroids at  $\approx 2$ – $20$  Myr after the breakup. They indicate that the impact rate at  $\approx 20$  Myr may have dropped by a factor of  $\sim 10$  from the initial value.

Unfortunately, their study provides little insight about the impact rate expected at  $\gtrsim 20$  Myr after the breakup because it ignores the important effects of collisions and Yarkovsky thermal drag, and the numerical integrations were not run long enough to span an adequate time interval. Additional work will be required to determine whether it is plausible that the impact rate of Flora meteoroids has dropped by about two orders of magnitude since 470 Ma as inferred from the number of fossil and recent  $L$ -chondrite meteorite falls (Schmitz et al., 2001).

<sup>5</sup> We assume here that the recovered fossil meteorites represent a large fraction of meteorites that were originally deposited in the analyzed quarry. In fact, many small fossil meteorites may have been lost due to terrestrial erosion/other processes (e.g., periods of fast covering by sediments may be needed to preserve fossil meteorites) or may have been overlooked in the sediments. Unfortunately, it is unclear how important these effects are and how they should be included in the above comparison.

The link between the  $L$  chondrites and Flora family is further supported by the results of Vokrouhlický and Farinella (2000) who showed that the range of measured CRE ages of recent  $L$ -chondrite meteorites ( $\sim 10$ – $100$  Myr; e.g., Marti and Graf, 1992) can be nicely matched if it is assumed that these meteorites are delivered from the Flora family region by the 3-step process described in the introduction. On the other hand, the spectral diversity of asteroids in the Flora family region has been usually taken as an evidence that not all dynamical members of the family can be linked to a single parent body. Indeed, as understood only recently, a large C/X-complex asteroid has disrupted in this region at 100–150 Ma producing the so-called Baptistina family, which overlaps in orbital space with the original Flora family. Therefore, the collisional history of this region has been complex and includes C/X type asteroid fragments that are unrelated to the 470-Ma breakup.

Additional constraints on the source of  $L$ -chondrite meteorites come from the analysis of chromite grains that were found in several quarries in Sweden (Schmitz et al., 2001, 2003; Schmitz and Häggström, 2006; see also Häggström, 2006 for a review). The mineral chromite ( $\text{FeCr}_2\text{O}_4$ ) is the most common oxide in most equilibrated ordinary chondrites (hereafter OCs). The recovered chromite grains have chemical composition very similar to the dominant type of chromite in the equilibrated OCs indicating their extraterrestrial origin. In short, the studies of recovered chromite grains at different locations and in different sediment layers showed that: (1) the enhanced flux of OC meteorites at  $\approx 470$  Ma was probably a global event affecting meteorite falls all over the Earth's surface; and (2) the enhanced meteorite flux started sharply at the time epoch represented by the Arkeologen bed in the Thorsberg quarry (Schmitz et al., 2001) and remained at high levels for at least  $\sim 10$  Myr after that epoch (Schmitz and Häggström, 2006).<sup>6</sup> Improved modeling will be required to match constraint (2). This modeling will need to include effects of collisions and extend the studied impact history over a longer time span than the one considered in this work.

<sup>6</sup> Most fossil meteorites were found in the 62 cm thick Arkeologen bed in the 3.2 m limestone sequence of the active Thorsberg quarry. The quarried interval represents 1–2 Myr of sedimentation, based on an average sedimentation rate of 2 mm per 1000 years (Schmitz et al., 2001). In the Arkeologen bed, 87 sediment dispersed chromite grains have been found in 26 kg of analyzed material, which comes to  $\approx 3.3$  chromite grains per kg (Schmitz et al., 2003). The total of 379 kg of material were analyzed below the Arkeologen bed resulting in 5 found grains, which comes to only  $\approx 0.013$  grain/kg (only  $\approx 0.4\%$  of the Arkeologen-bed chromite grain density). Chromite grain searches were also performed on samples collected 4.2 and 8.5 m above the Arkeologen bed. In 4.2 m above, 31 chromite grains were found in 14 kg of material. This represents  $\approx 2.2$  grain/kg. In 8.5 m above, 11 chromite grains were found in 4.5 kg of material. This represents  $\approx 0.4$  grain/kg. The time separation between the Arkeologen bed and samples analyzed in sediments 4.2 and 8.5 m above the Arkeologen bed is probably several Myr and  $\sim 10$  Myr, respectively. These results document the sharp start of the enhanced meteorite flux at  $\approx 470$  Ma (chromite grain density steps up from 0.013 to 3.3 grain/kg) and its slow decay within during the subsequent  $\sim 10$  Myr (chromite grain density decreases by a factor of a few). The slow decay of meteorite falls inferred from the collected chromite grains was not yet documented by findings of fossil meteorites in sediments above the Arkeologen bed because these small meteorites are extremely difficult to find outside the active quarry.

## Acknowledgments

This paper is based upon work supported by the NASA PG&G program (Grant No. 513038). The work of D.V. was partially supported by the Czech Grant Agency (Grant No. 205/05/2737). B.G. thanks CFI, BCKDF, and NSERC for financial support. We thank A. Morbidelli, P.R. Heck, and an anonymous referee for their very useful suggestions to this work.

## References

- Bertotti, B., Farinella, P., Vokrouhlický, D., 2003. Physics of the Solar System. Kluwer Academic, Dordrecht.
- Bogard, D.D., 1995. Impact ages of meteorites: A synthesis. *Meteoritics* 30, 244–268.
- Bogard, D.D., Wright, R.J., Husain, L., 1976. Ar-40/Ar-39 dating of collisional events in chondrite parent bodies. *J. Geophys. Res.* 81, 5664–5678.
- Borovička, J., Kalenda, P., 2003. The Morávka meteorite fall. 4. Meteoroid dynamics and fragmentation in the atmosphere. *Meteorit. Planet. Sci.* 38, 1023–1043.
- Bottke, W.F., Nolan, M.C., Greenberg, R., Kolvoord, R.A., 1994. Velocity distributions among colliding asteroids. *Icarus* 107, 255–268.
- Bottke, W.F., Vokrouhlický, D., Brož, M., Nesvorný, D., Morbidelli, A., 2001. Dynamical spreading of asteroid families via the Yarkovsky effect. *Science* 294, 1693–1696.
- Bottke, W.F., Morbidelli, A., Jedicke, R., Petit, J., Levison, H.F., Michel, P., Metcalfe, T.S., 2002. Debiased orbital and absolute magnitude distribution of the near-Earth objects. *Icarus* 156, 399–433.
- Bottke, W.F., Durda, D., Nesvorný, D., Jedicke, R., Morbidelli, A., Levison, H.F., 2005a. The fossilized size distribution of the main asteroid belt. *Icarus* 175, 111–140.
- Bottke, W.F., Durda, D., Nesvorný, D., Jedicke, R., Morbidelli, A., Vokrouhlický, D., Levison, H.F., 2005b. Linking the collisional history of the main asteroid belt to its dynamical excitation and depletion. *Icarus* 179, 63–94.
- Bottke, W.F., Vokrouhlický, D., Rubincam, D.P., Nesvorný, D., 2006. The Yarkovsky and YORP effects: Implications for asteroid dynamics. In: Jeanloz, R. (Ed.), Annual Review of Earth and Planetary Sciences. Annual Reviews, Palo Alto, CA, pp. 157–191.
- Brouwer, D., Clemence, G.M., 1961. Methods of Celestial Mechanics. Academic Press, New York.
- Bus, S.J., Binzel, R.P., 2002. Phase II of the small main-belt asteroid spectroscopic survey. A feature-based taxonomy. *Icarus* 158, 146–177.
- Caffee, M.W., Reedy, R.C., Goswami, J.N., Hohenberg, C.M., Marti, K., 1988. Irradiation records in meteorites. In: Meteorites and the Early Solar System. Univ. of Arizona Press, Tucson, pp. 205–245.
- Cellino, A., Bus, S.J., Doressoundiram, A., Lazzaro, D., 2002. Spectroscopic properties of asteroid families. In: Bottke, W.F., Cellino, A., Paolicchi, P., Binzel, R. (Eds.), Asteroids III. Univ. of Arizona Press, Tucson, pp. 633–643.
- Cepelka, Z., Revelle, D.O., 2005. Fragmentation model of meteoroid motion, mass loss, and radiation in the atmosphere. *Meteorit. Planet. Sci.* 40, 35.
- Dohnanyi, J.W., 1969. Collisional models of asteroids and their debris. *J. Geophys. Res.* 74, 2531–2554.
- Dones, L., Gladman, B., Melosh, H.J., Tonks, W.B., Levison, H.F., Duncan, M., 1999. Dynamical lifetimes and final fates of small bodies: Orbit integrations vs Öpik calculations. *Icarus* 142, 509–524.
- Durda, D.D., Bottke, W.F., Nesvorný, D., Enke, B.L., Merline, W.J., 2006. Size-frequency distributions of fragments from SPH/N-body simulations of asteroid impacts: Comparison with observed asteroid families. *Icarus*, in press.
- Farinella, P., Froeschlé, C., Froeschlé, Ch., Gonczi, R., Hahn, G., Morbidelli, A., Valsecchi, G.B., 1994. Asteroids falling onto the Sun. *Nature* 371, 315–317.
- Farley, K.A., Vokrouhlický, D., Bottke, W.F., Nesvorný, D., 2006. A late Miocene dust shower from the break-up of an asteroid in the main belt. *Nature* 439, 295–297.
- Gaffey, M.J., 1984. Rotational spectral variations of Asteroid (8) Flora implications for the nature of the S-type asteroids and for the parent bodies of the ordinary chondrites. *Icarus* 60, 83–114.
- Gaffey, M.J., Burbine, T.H., Piatek, J.L., Reed, K.L., Chaky, D.A., Bell, J.F., Brown, R.H., 1993. Mineralogical variations within the S-type asteroid class. *Icarus* 106, 573–602.
- Gladman, B.J., Migliorini, F., Morbidelli, A., Zappalà, V., Michel, P., Cellino, A., Froeschlé, C., Levison, H.F., Bailey, M., Duncan, M., 1997. Dynamical lifetimes of objects injected into asteroid belt resonances. *Science* 277, 197–201.
- Graf, T., Marti, K., 1994. Collisional records in LL-chondrites. *Meteoritics* 29, 643–648.
- Haack, H., Farinella, P., Scott, E.R.D., Keil, K., 1996. Meteoritic, asteroidal, and theoretical constraints on the 500 Ma disruption of the L-chondrite parent body. *Icarus* 119, 182–191.
- Häggström, T., 2006. Extraterrestrial chromite as tracer of ancient meteorite flux—Evidence from condensed Middle Ordovician limestone in southern Sweden. Thesis, Department of Earth Sciences Centre, Göteborg University.
- Heck, P.R., Schmitz, B., Baur, H., Halliday, A.N., Wieler, R., 2004. Fast delivery of meteorites to Earth after a major asteroid collision. *Nature* 430, 323–325.
- Heymann, D., 1967. On the origin of hypersthene chondrites: Ages and shock effects of black chondrites. *Icarus* 6, 189–221.
- Hirayama, K., 1918. Groups of asteroids probably of common origin. *Astron. J.* 31, 185–188.
- Keil, K., Haack, H., Scott, E.R.D., 1994. Catastrophic fragmentation of asteroids: Evidence from meteorites. *Planet. Space Sci.* 42, 1109–1122.
- Korochantseva, E.V., Trieloff, M., Buikin, A.I., Lorenz, C.A., Ivanova, M.A., Schwarz, W.H., Hopp, J., Jessberger, E.K., 2006. L-chondrite asteroid breakup tied to Ordovician meteorite shower by multiple isochron  $^{40}\text{Ar}$ – $^{39}\text{Ar}$  dating. In: Proceedings of 69th Annual Meeting of the Meteoritical Society, held August 6–11, 2006 in Zurich, Switzerland. *Meteorit. Planet. Sci. Suppl.* 41, 5087.
- Levison, H.F., Duncan, M.J., 1994. The long-term dynamical behavior of short-period comets. *Icarus* 108, 18–36.
- Marti, K., Graf, T., 1992. Cosmic-ray exposure history of ordinary chondrites. *Annu. Rev. Earth Planet. Sci.* 20, 221–243.
- Michel, P., Benz, W., Tanga, P., Richardson, D., 2001. Collisions and gravitational reaccumulation: A recipe for forming asteroid families and satellites. *Science* 294, 1696–1700.
- Michel, P., Tanga, P., Benz, W., Richardson, D.C., 2002. Formation of asteroid families by catastrophic disruption: Simulations with fragmentation and gravitational reaccumulation. *Icarus* 160, 10–23.
- Milani, A., Knežević, Z., 1994. Asteroid proper elements and the dynamical structure of the asteroid main belt. *Icarus* 107, 219–254.
- Morbidelli, A., Gladman, B., 1998. Orbital and temporal distributions of meteorites originating in the asteroid belt. *Meteorit. Planet. Sci.* 33, 999–1016.
- Morbidelli, A., Henrard, J., 1991. The main secular resonances  $\nu_6$ ,  $\nu_5$ , and  $\nu_{16}$  in the asteroid belt. *Celest. Mech. Dynam. Astron.* 51, 169–197.
- Morbidelli, A., Nesvorný, D., 1999. Numerous weak resonances drive asteroids toward terrestrial planets orbits. *Icarus* 139, 295–308.
- Morbidelli, A., Nesvorný, D., Bottke, W.F., Michel, P., Vokrouhlický, D., Tanga, P., 2003. The shallow magnitude distribution of asteroid families. *Icarus* 162, 328–336.
- Mothé-Diniz, T., Roig, F., Carvano, J.M., 2005. Reanalysis of asteroid families structure through visible spectroscopy. *Icarus* 174, 54–80.
- Nakamura, A.M., 1993. Laboratory Studies on the Velocity of Fragments from Impact Disruptions. Institute of Space and Astronautical Science, Tokyo. ISAS Report 651.
- Nesvorný, D., Morbidelli, A., Vokrouhlický, D., Bottke, W.F., Brož, M., 2002a. The Flora family: A case of the dynamically dispersed collisional swarm? *Icarus* 157, 155–172.
- Nesvorný, D., Bottke, W.F., Levison, H., Dones, L., 2002b. A recent asteroid breakup in the main belt. *Nature* 417, 720–722.
- Nesvorný, D., Jedicke, R., Whiteley, R.J., Ivezić, Ž., 2005. Evidence for asteroid space weathering from the Sloan Digital Sky Survey. *Icarus* 173, 132–152.

- Nesvorný, D., Bottke, W.F., Vokrouhlický, D., Morbidelli, A., Jedicke, R., 2006a. Asteroid families. IAU Symposium 229, 289–299.
- Nesvorný, D., Enke, B.L., Bottke, W.F., Durda, D.D., Asphaug, E., Richardson, D.C., 2006b. Karin cluster formation by asteroid impact. *Icarus* 183, 296–311.
- Öpik, E.J., 1951. Collision probabilities with the planets and the distribution of interplanetary matter. *Proc. R. Irish Acad.* 54, 165–199.
- Schmitz, B., Häggström, T., 2006. Extraterrestrial chromite in Middle Ordovician marine limestone at Kinnekulle, southern Sweden—Traces of a major asteroid breakup event. *Meteorit. Planet. Sci.* 41, 455–466.
- Schmitz, B., Lindström, M., Asaro, F., Tassinari, M., 1996. Geochemistry of meteorite-rich marine limestone strata and fossil meteorites from the lower Ordovician at Kinnekulle, Sweden. *Earth Planet. Sci. Lett.* 145, 31–48.
- Schmitz, B., Peucker-Ehrenbrink, B., Lindström, M., Tassinari, M., 1997. Accretion rates of meteorites and cosmic dust in the Early Ordovician. *Science* 278, 88–90.
- Schmitz, B., Tassinari, M., Peucker-Ehrenbrink, B., 2001. A rain of ordinary chondritic meteorites in the Early Ordovician. *Earth Planet. Sci. Lett.* 194, 1–15.
- Schmitz, B., Häggström, T., Tassinari, M., 2003. Sediment-dispersed extraterrestrial chromite traces a major asteroid disruption event. *Science* 300, 961–964.
- Sears, D.W.G., Dodd, R.T., 1988. Overview and classification of meteorites. In: Kerridge, J.F., Matthews, M.S. (Eds.), *Meteorites and the Early Solar System*. Univ. of Arizona Press, Tucson, pp. 3–31.
- Šídlichovský, M., Nesvorný, D., 1997. Frequency modified Fourier transform and its applications to asteroids. *Celest. Mech. Dynam. Astron.* 65, 137–148.
- Smith, B.A., Goldstein, J.I., 1977. The metallic microstructures and thermal histories of severely reheated chondrites. *Geochim. Cosmochim. Acta* 41, 1061–1065.
- Turner, G., 1969. Thermal histories of meteorites by the  $^{39}\text{Ar}$ – $^{40}\text{Ar}$  method. In: Millman, P.M. (Ed.), *Meteorite Research*. In: *Astrophysics and Space Science Library*, vol. 12. Reidel, Dordrecht, p. 407.
- Turner, G., 1988. Dating of secondary events. In: Kerridge, J.F., Matthews, M.S. (Eds.), *Meteorites and the Early Solar System*. Univ. of Arizona Press, Tucson, pp. 276–288.
- Vokrouhlický, D., Farinella, P., 2000. Efficient delivery of meteorites to the Earth from a wide range of asteroid parent bodies. *Nature* 407, 606–608.
- Vokrouhlický, D., Brož, M., Morbidelli, A., Bottke, W.F., Nesvorný, D., Lazzaro, D., Rivkin, A.S., 2006a. Yarkovsky footprints in the Eos family. *Icarus* 182, 92–117.
- Vokrouhlický, D., Brož, M., Bottke, W.F., Nesvorný, D., Morbidelli, A., 2006b. Yarkovsky/YORP chronology of asteroid families. *Icarus* 182, 118–142.
- Welten, K.C., Lindner, L., van der Borg, K., Loeken, T., Scherer, P., Schultz, L., 1997. Cosmic-ray exposure ages of diogenites and the recent collisional history of the HED parent body/bodies. *Meteorit. Planet. Sci.* 32, 891–902.
- Wetherill, G.W., 1967. Collisions in the asteroid belt. *J. Geophys. Res.* 72, 2429–2444.
- Wetherill, G.W., Williams, J.G., 1979. Origin of differentiated meteorites. In: *Origin and Distribution of the Elements*. Pergamon Press, London, pp. 19–31.
- Wisdom, J., 1982. The origin of the Kirkwood gaps—A mapping for asteroidal motion near the 3/1 commensurability. *Astron. J.* 87, 577–593.
- Wisdom, J., 1985. Meteorites may follow a chaotic route to Earth. *Nature* 315, 731–733.
- Wisdom, J., Holman, M., 1991. Symplectic maps for the  $N$ -body problem. *Astron. J.* 102, 1528–1538.
- Zappalà, V., Cellino, A., Gladman, B.J., Manley, S., Migliorini, F., 1998. Note: Asteroid showers on Earth after family breakup events. *Icarus* 134, 176–179.